Current Photovoltaic Research 4(2) 31-41 (2016)
DOI:http://dx.doi.org/10.21218/CPR.2016.4.2.031
pISSN 2288-3274
eISSN 2508-125X

Optimization of the Phosphorus Doped BSF Doping Profile and Formation Method for N-type Bifacial Solar Cells

Jian Cui[1)] · Shihyun Ahn[1)] · Nagarajan Balaji[2)] · Cheolmin Park[2)] · Junsin Yi[1,2)]*

[1)]College of Information and Communication Engineering, Sungkyunkwan University, Suwon 16419, Korea
[2)]Department of Energy Science, Sungkyunkwan University, Suwon 16419, Korea

ABSTRACT: n-type PERT (passivated emitter, rear totally diffused) bifacial solar cells with boron and phosphorus diffusion as p+ emitter and n+ BSF (back surface field) have attracted significant research interest recently. In this work, the influences of wafer thickness, bulk lifetime, emitter, BSF on the photovoltaic characteristics of solar cells are discussed. The performance of the solar cell is determined by using one-dimensional solar cell simulation software PC1D. The simulation results show that the key role of the BSF is to decrease the surface doping concentration reducing the recombination and thus, increasing the cell efficiency. A lightly phosphorus doped BSF (LD BSF) was experimentally optimized to get low surface dopant concentration for n type bifacial solar cells. Pre-oxidation combined with a multi-plateau drive-in, using limited source diffusion was carried out before pre-deposition. It could reduce the surface dopant concentration with minimal impact on the sheet resistance.

Key words: N-type, Bifacial silicon solar cell, BSF, Diffusion, PC1D simulation

1. INTRODUCTION

Looking back to the history of solar cell, the first modern solar cell was invented in 1954 at the Bell Laboratories and was based on As doped silicon with a rear contact[1)]. In the early days, the solar cells were too expensive for common use and they were only used for space applications. It was then found that p-type cells showed higher radiation hardness than n-type solar cells in the space radiation environment. Accordingly the research focus shifted towards cells based on boron or gallium doped p-type silicon. It is this early focus on manufacturing techniques for p-type cells that is partly responsible for the dominating position of p-type solar cells in the industry today.

An aluminum back surface field (Al-BSF) created by a co-fired screen-printed method and front side doped with phosphorus results in the currently dominating mono-crystalline and multi-crystalline silicon solar cell structures. Although the photovoltaic industry is mainly occupied by p-type also at the current stage of development, it seems that p-type efficiencies have saturated. Many researchers have acknowledged betterr suitability of n-type CZ-material for solar cell to get higher efficiencies[2-4)]. It is expected a growth in shares for n-type silicon substrates, as interest in using n-type silicon substrates has increased recently. The 2015 edition of the international technology road map for photovoltaics (ITRPV) also predicts a clear shift from p-type to n-type substrates in the market shares of monocrystalline silicon (Fig. 1, 2). This expected shift in the solar cell module technology is because of certain significant advantages of n-type silicon over p-type silicon substrates for solar cell fabrication.

Compared to standard p-type silicon solar cells, the most important advantage offered by n-type silicon is the absence of boron oxygen-related (B-O pairs), light-induced degradation (LID). It has already been reported that the boron oxygen pair formation causes degradation in carrier life time for c-Si solar cells based on p-type CZ c-Si[5-7)]. The absence of the boron in phosphorus-doped n-type substrates eliminates the boron oxygen defects even for the higher oxygen concentration. Furthermore, the n-type material exhibits enough strength against common impurities, such as interstitial Fe, which can capture the electrons much more effectively as it has a positive charge state[8)]. The minority carriers in n-type silicon are holes instead of electrons as in the case of p-type silicon; therefore, it offers higher minority carrier diffusion lengths as compared to p-type c-Si substrates with similar impurity concentrations. Moreover, the use of a phosphorus-doped back surface field (BSF) with convenient surface passivation for such n-type cells, results in higher diffusion

*Corresponding author: yi@yurim.skku.ac.kr
Received December 24, 2015; Revised January 4, 2016; Accepted January 7, 2016

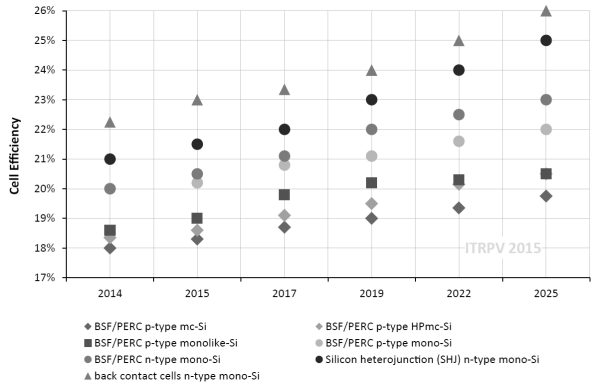

Fig. 1. Average stabilized efficiency values for Si solar cells

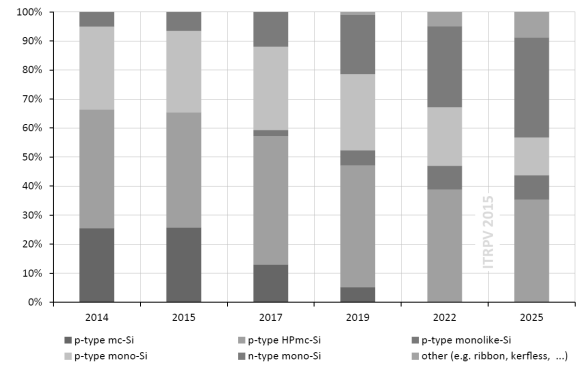

Fig. 2. World market shares for different wafer types

depth and better rear internal reflection. The use of a boron-doped front emitter with rear side phosphorus doped BSF on n-type substrates offers a bifacial type cell structure which can be fabricated on thinner wafers. The convenience of making such bifacial designed solar cells and modules using phosphorus-doped BSF also generates opportunities to produce cells with higher efficiencies.

BSF as a part of a bifacial solar cell has been shown to have a significant influence on solar cell efficiency. But very little systematic analysis on the influence of BSF doping profile on cell efficiency exists. Gaining higher lateral conductivity by stronger BSF doping and decreasing BSF sheet resistance is a well-known method to increase FF (Fill Factor). However, there is a trade-off between Voc and Isc due to higher Auger- and surface recombination. In this work, we also investigate the optimizing of the phosphorus BSF profile. Not only has the depth but also surface as well as peak concentration played an important role.

In this work, a lightly doped BSF (LD BSF) method was achieved by optimizing the doping profile to result in a lower surface dopant concentration by a pre-oxidation combined with a multi-plateau drive-in using limited source diffusion was carried out before pre-deposition. It could reduce the surface dopant concentration with minimal impact on the sheet resistance. The phosphorus-doped BSF formation for n-type PERT solar cells was investigated. The recombination problems (in particular on the recombination at the silicon/metal contacts) were investigated by changing the BSF formation[9-10] and the contacts were optimized.

2 Applied N-type Cell Structure overviews

Currently, p-type solar cell architectures are mostly limited by bulk recombination from the metastable boron oxygen defect. For advanced cell concepts the bulk limitation has to be overcome. The magnetic CZ is a method to reduce the influence of this defect by reducing the oxygen concentration in the crystal but it is too expensive to use these days. In addition, the substitution of boron by gallium is discussed, but it leads to very large resistivity and interstitial iron would cause degradation.

Although the boron oxygen defect would remain, the sensitivity of p-type for common metal impurities is higher than that of n-type material due to asymmetric capture cross sections of their defects[11]. This could still be the limiting factor for the bulk lifetime. However this highly quoted assumption should be taken with care. On n-type cells with boron emitter even higher cleanliness requirements might apply since the boron diffusion is sensitive towards emitter bulk contamination. Even though the bulk might limit high efficiency, the recombination within a contaminated p+ emitter can easily destroy the cell performance[12]. Every p-type module installed today suffers from light induced degradation (LID), which reduces power output substantially over the working life of a module. This effect is fully negligible in cells made from non-compensated n-type silicon. Today it is taken as normal by an installer, that the energy output of a Si-module diminishes over its working life, simply because p-type modules have been the only type available. The stable performance will certainly be a major advantage for all kinds of n-type devices, but it will require marketing efforts. Many n-type cell concepts are moreover inherently bifacial. The module assembly can then be adjusted to make use of the bifacial properties, enabling new ways of installation in the field but also for building integrated photovoltaic. Last but not least there is evidence that n-type devices are more sensitive to low light intensity as well as having a lower temperature coefficient mostly due to the higher V_{OC}.

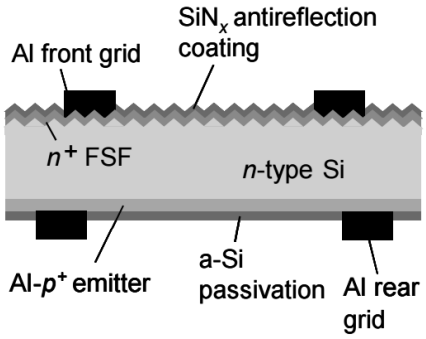

Fig. 3. N+ N P+ Al-rear emitter cells structure

2.1 Aluminum rear emitter cells

Aluminum rear emitter cell can be fabricated using the process sequence of standard p-type Al-BSF cells simply by starting with n-type CZ material because it is similar with aluminum BSF p-type solar cell. This makes the process appealing at first, since existing production lines can be re-fitted to produce this cell. The potential of the cell concept has been evaluated by Rudiger[13] and efficiencies of 19.4% on 6 inch wafers have been demonstrated by Book et al.[14]. Basically, the benefits over its p-type equivalent are limited. The poor electrical properties of a full area aluminum emitter limit the cell V_{OC} and the internal optical properties put an upper bound on the achievable cell current density Jsc (Fig. 3).

2.2 PERC, PERL and PERT cells

Recent high efficiency solar cell cannot be imagined without emitter passivation, the rear surface, however, much looks like it did since the aluminum BSF was invented. An advanced line of cell concepts deals with improving the rear surface compared to aluminum BSF cells. The PERC (passivated emitter and rear cell) is gradually being adopted by the industry adding rear side passivation to the structure. As rear side dielectric commonly Al2O3 is employed. The rear side is opened locally usually by laser ablation, to allow for local alloying of aluminum. This forms the BSF and contacts, thus improving the recombination and optical properties. Accordingly the PERC concept has been promoted for many years as the next candidate for widespread industrial implementation. By now initial efficiencies exceeding 20% have been demonstrated by many manufacturers. This approach cannot easily be transferred to n-type cells. In case of a PERL (passivated emitter, rear locally diffused) cell this is refined even further by diffusing a local BSF, which is contacted by evaporated and plated metal contacts. The long-standing efficiency world record for silicon devices was established using such a structure. Zhao[15] reported 24.7% on a designated area of 4 cm^2 on FZ p-type wafers. This is achieved by combining all cell design ingredients necessary for achieving highest efficiencies. Those include selective front doping, ideal inverted pyramid texture with double layer anti-reflection coating, an evaporation coated rear side for improved light trapping and front contacts structured by photolithography. Using a process of similar complexity 23.4% efficiency has been shown for 4 cm^2 n-type PERL devices by Benick[16,17]. Needless to say, these processes are too complicated and costly for mass production. The direct contender of the p-type PERC cell in the race for industrial implementation can be found in the n-type PERT (passivated emitter, rear totally diffused) cell discussed in this work. These can be fabricated with front emitter or as back junction cells with an emitter on the rear side. The best lab results for front junction n-PERT devices have been reported by Zhao[18] with 21.1% on small area CZ and 21.9% on FZ material. Newer experimental results using Al_2O_3-based passivation were reported by Richter et al.[19], who could demonstrate 20.5% on 4 cm2 FZ cells with a p+nn+ structure using advanced metallization techniques. On 5 inch CZ-material still 19.6% has been shown by on back junction devices with rear boron emitter have been pioneered by Q-Cells/ Hanhwa as reported from Bordihn et al[20]. In a recent update by Mertens[21] efficiencies up to 21.3% on large area CZ based solar cells have been shown, using PVD aluminum metallization on the rear side. Several research groups with a focus on industrial implementation are currently working on the front emitter version of this cell concept. ECN is promoting this concept under the name n-Pasha (towards 20%) and attempts to merge the concepts with metal wrap through (MWT) technology have been successfully demonstrated. Also in France, at CEAINES these cell types are being developed, recently the efficiency of 20.1% was reported[22]. Both share the formation of doped layers with conventional tube diffusions, passivation by aluminum oxide or nitric acid oxide based passivation stacks and industrial screen-printing. The advent of ion implantation for solar cell manufacturing also has implications for the process sequences of n-PERT cells. BOSCH Solar Energy AG reported n-PERT results from pilot line production of up to 20.6% using implanted phosphorous BSF structures[23].

2.3 Heterojunction cells

A new structure of devices that combines the advantages of n-type bulk material and semiconductor grade passivation are heterojunction structures. Here a high quality n-type substrate is

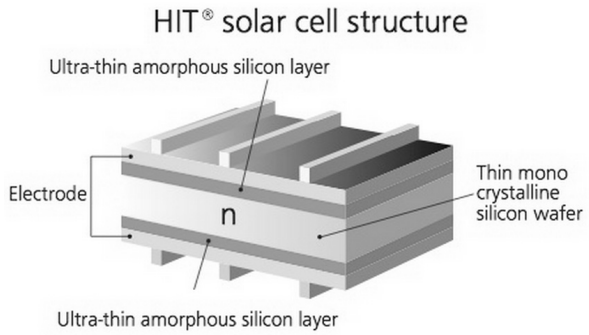

Fig. 4. HIT solar cell structure

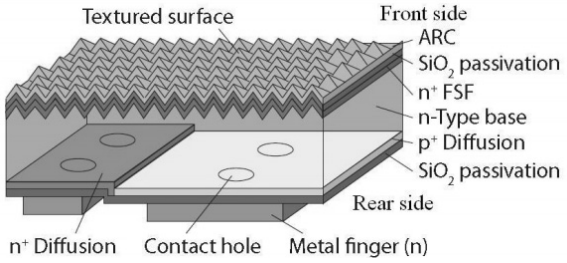

Fig. 5. IBC solar cell structure from SunPower

coated with stacks of intrinsic and doped amorphous silicon to give a p+ i n i n+ structure. The wafer is coated on either side with indium tin oxide (ITO) to enhance current collection from the contacts. The a-Si enables superb passivation of the bulk silicon and enables a tunneling junction to the doped emitter layer. This results in extremely high voltage potential and low temperature coefficients. The cost benefit of low temperature deposition for the amorphous layers leads to the requirement of exceptionally high bulk lifetime. Additionally the low temperature processing forbids the use of firing through metallization. The commonly employed low temperature contact pastes show significantly larger resistances compared to their sintered counterparts. Despite these drawbacks very high efficiencies have been demonstrated by several companies. The most famous example certainly is the concept of heterojunction cells with intrinsic thin layer (HIT) from Panasonic, initially from Sanyo. The certified peak efficiency was just raised by one percent absolute to 24.7% for a 100 mm thick cell on 101.8 cm^2. One competitor, Kaneka, reported a certified efficiency of 24.2% on large area cells, using copper plated contacts at the same time. These results demonstrate the very high efficiency potential of this concept. It is expected that average production efficiencies range 1-2% lower than the best cell efficiencies in the research environment. Cell concepts combine an n-type silicon bulk, with an amorphous silicon emitter. This heterojunction architecture enables over 730 mV in V_{OC}. A semiconductor grade tunneling oxide is deposited on top, forming a tunneling contact to the copper plated metallization. Peak efficiencies of 22.1% have been demonstrated on 239 cm^2. An average production efficiency of 21.3% was also reported[24] (Fig. 4).

2.4 IBC cells

The interdigitated back contact (IBC) cell concept is characterized in that all metal contacts can be found on the rear side of the cell. This enables a front side optimized entirely for higher light absorption without the requirements of contact formation. Since the contacts are all on the rear side, the contact layout can be optimized for transport properties irrespective of shading considerations. These advantages stand in opposition to higher process complexity due the requirement of patterned diffusions and the risk of fatal cell shunting due to the proximity of n+ and p+ doped regions. For back-contact back junction designs high bulk lifetime is further required to achieve highest efficiencies as analyzed by Granek. This structure can also be fabricated using the aluminum emitter, but will then suffer from the same limitations. A report on the status of development for this cell is given in Ref[25]. The most prominent example for IBC cells comes from the company Sun power Corp. With a rated maximum efficiency of 24.2% and a reported average production efficiency of 23.6% their implementation of the IBC concept stands out from the range of commercially available silicon solar cells[26]. These results are achieved on 5 inch wafers and employing a very complex production sequence (Fig. 5).

2.5 TOPCon cells

Due to the improvement in material quality and surface passivation, high efficiency solar cells are often limited by the recombination at the metal semiconductor contacts. A solution called the TOPCon (Tunnel Oxide Passivated Contact) technology, developed by Fraunhofer ISE, metal contacts are applied to the rear side without patterning. To achieve this, researchers developed a selective passivated contact made of tunnel oxide that enables majority carriers to pass and prevents the minority carriers from recombining. The thickness of the intermediate passivation layer is reduced to one or two nanometers, allowing the charge carriers to “tunnel” through it. Subsequently, a thin coating of highly doped silicon is deposited over the entire layer of ultra-thin tunnel oxide. This novel combination of layers allows electrical current to flow out of the cell with nearly zero loss. An efficiency of 25.1% has been measured for a both sides contacted

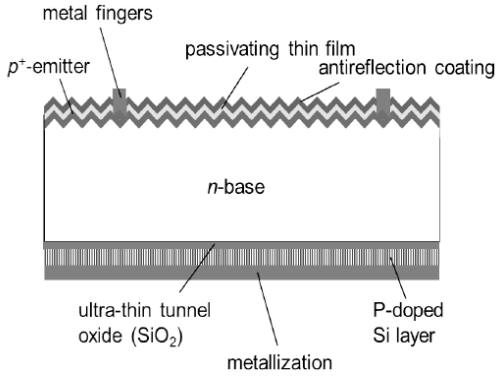

Fig. 6. TOPCon solar cell structure

silicon solar cell. Having a simple rear side contact without any patterning, this type of solar cell converts one quarter of the incident sunlight into electricity. The new concept for the solar cell rear side holds great potential for further increases in efficiency (Fig. 6)[27].

3. Potential of N-type bifacial solar cell in PC1D device simulations

PC1D computer program is a widely used numerical modeling program for simulation of crystalline semiconductor solar cells. It uses a finite-element numerical method for solving the coupled nonlinear equations for carrier generation, recombination and transport in the device. It can be widely used for simulation of device performance. The advantages of using PC1D are high calculation speeds, broad list of material and physical parameters and an instinctive user interface. PC1D can be used to calculate the current-voltage characteristics and spectral quantum efficiency of the solar cell. It also has a large number of options for analysis both in time domain and spatial domain. The circuit evaluation lacks accuracy because it cannot account for in homogeneities in the sheet resistance or contact resistance which can have a detrimental influence on the cell voltage and fill factor. Anyhow series and parallel resistance are implemented in the simulation as a lumped number extracted from the best cell results. They are therefore small enough not to have any detrimental effect on the V_{OC} or J_{SC}. The PC1D computer program is limited to one-dimensional modeling. Batch mode of PC1D allows to rapidly perform optimization study for a particular parameter rather than varying the parameters frequently. In batch mode, for each input parameter, the range to be varied over, the number of different values and type of variations (logarithmically or linearly) are to be specified. The doping profiles are approximated by error functions which give the best fit to experimental data. But it is not the same shape of the doping profiles. Especially the peak surface concentrations for the simulated profiles are overestimated, which reduces the cell potential. Design of this work was optimized with PC1D Version 5.9 simulation program. It includes a device schematic, which reflects the changing of device structure and parameters, such as texture, doping, external elements and etc. The influence of various parameters such as series and parallel resistance, emitter and BSF doping, bulk lifetime, minority carrier lifetime, wafer thickness, front and rear surface recombination and illumination from front and rear surfaces were investigated by PC1D. It was found that minority carrier lifetime and wafer thickness are critical parameters to bifacial solar cell performance.

1. Influence of the wafer thickness
2. Influence of the bulk lifetime (Effects in the bulk (Auger, SRH, radiative)
3. Influence of the emitter doping profile and passivation
4. Influence of the BSF doping profile and passivation

3.1 Influence of the wafer thickness

Although the decrease in the wafer thickness is a very effective way for saving the fabrication cost of the solar cell, thinner Si

Table 1. PC1D simulation parameters

Parameter	Input
Material	Silicon
Device area	100 cm^2
pyramid height (Both)	3 μm/54.74°
Internal reflection (Both)	95%
Series resistance	3 mΩ
Parallel resistance	10 kΩ
Cells thickness	170 μm
Bulk resistivity	3 Ωcm
Bulk lifetime (n & p)	1 ms
Front Diffusion: P-type	1E20 cm-3/0.6 μm
Rear Diffusion: N-type	1. E20 cm-3/0.48 μm
Bulk recombination	1000 μs
Surface recombination velocity (both)	5000 cm/s
Diode ideality	1
Metal shading	6%
Temperature	25°C
Base circuit	-0.8 to 0.8 V
Collector circuit	Zero
Constant intensity	0.1W/ cm^2
Spectrum	AM1.5

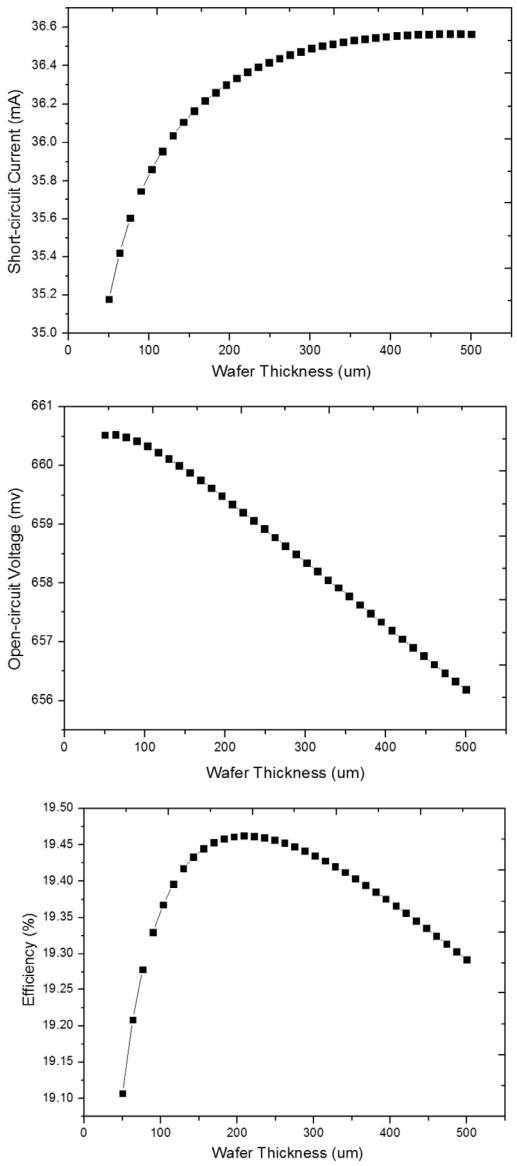

Fig. 7. PC1D simulation for cell performance depending on wafer thickness

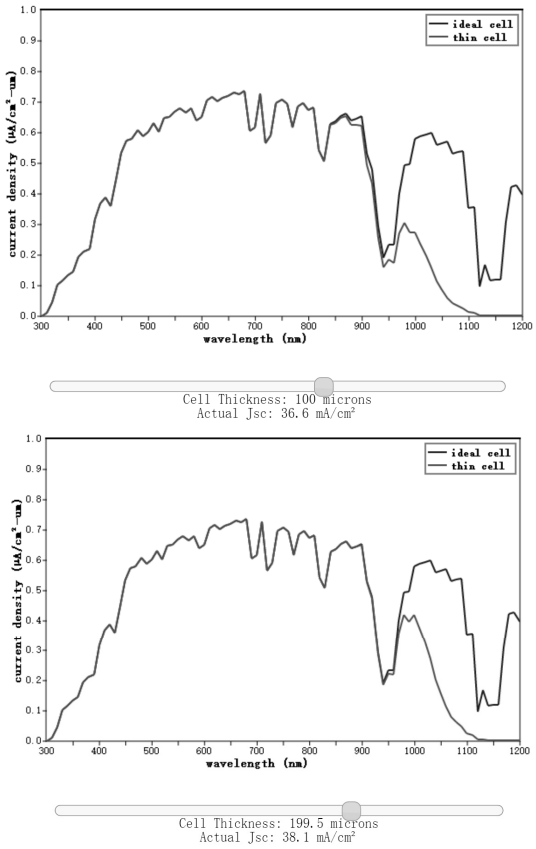

Fig. 8. 100 μm solar cells show a current density losses for long wavelengths compared to 200 μm cells corresponding to the Jsc loss

wafers also cause some problems. The first problem is a weakness in mechanical strength. A thin Si wafer is not only easily cracked but also very easily warped by mechanical and thermal stresses. The warping of the cell might cause a drop in the process yield for the solar module assembly process. The second problem is a decrease in photo-current. Because the absorption coefficient of Si in the near-infrared region is low, incident photons in the near-infrared wavelength penetrate the wafer without being absorbed into the Si. This causes a quickly decrease in I_{SC} when wafer thickness below 200 μm. From the simulation result, for wafer thicknesses < 200 μm the cell efficiency decreases strongly. This is caused by Jsc loss through insufficient light trapping. The simulated cell performance of thin cell is mainly influenced by short circuit current, Jsc. For wafer thickness < 200 um, light trapping becomes challenging and causes a steep decline in Jsc. This leads to the conclusion that the N type bifacial solar cell is suitable for about 200 μm thick wafer.

3.2 Influence of the bulk lifetime

Even for the best solar cell structure, it will not result in high efficiencies if the material quality is poor. Therefore the investigation of electrically active defects is very important for photovoltaic material. High amount of metal impurity and crystal defects will influence the bulk lifetime and SRV of front / rear sides and the cell performance will be limited by the bulk properties.

In this work for investigating the effect influenced by bulk properties, the front and back surface recombination velocity, S are varied from 0 to 5000 *cm/s* in the simulation. Bulk lifetime of c-Si wafer is varied while S is fixed from 0 to 5000 *cm/s*. The efficiency improves as bulk lifetime increases since carriers have less opportunity to be recombine. When the bulk lifetime below 300 us, it decreases very quickly.

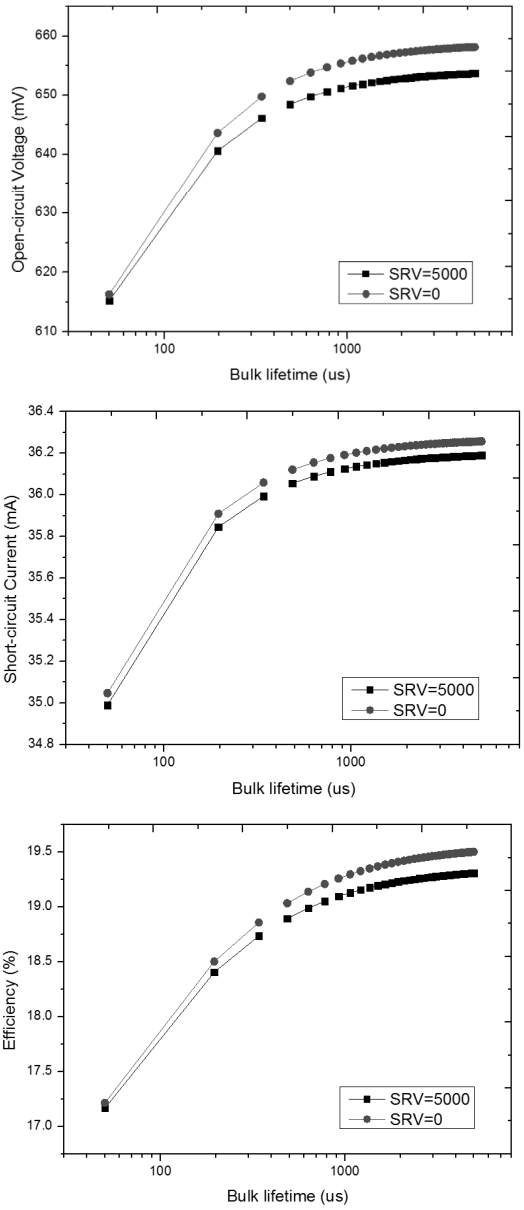

Fig. 9. PC1D simulation for cell performance dependence on wafer bulk lifetime

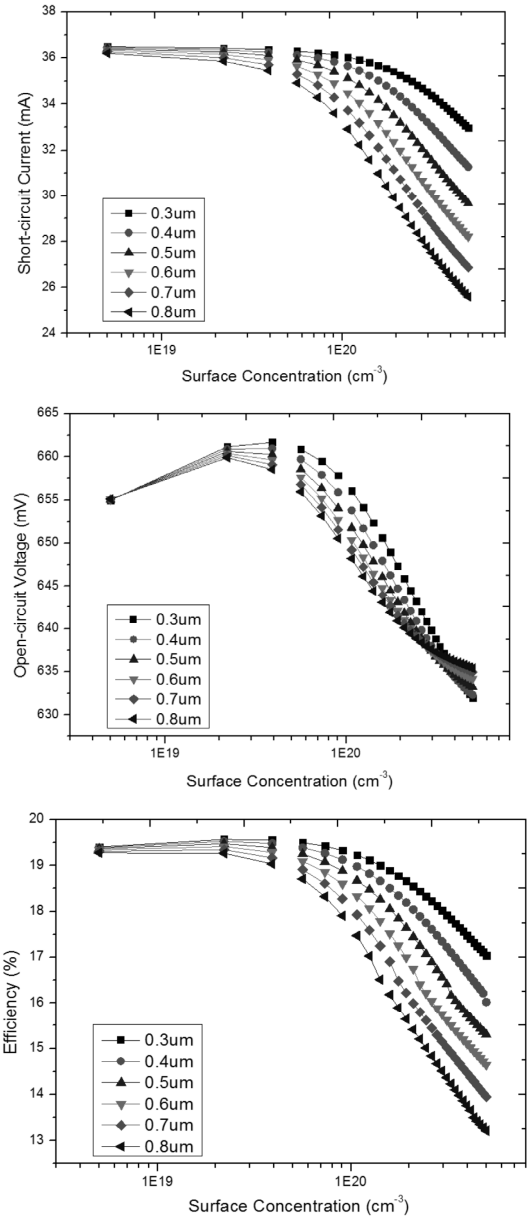

Fig. 10. PC1D simulation for cell performance depending on doping profiles of emitter

3.3 Influence of the emitter and BSF doping profile and passivation

From the result, it can be concluded that reducing the emitter doping immediately improves the current, due to less Auger recombination, and also gradually increases the voltage. If the front surface passivation (lower SRV) is improved at the same time, a drastic gain in V_{OC} can also be expected. It can be seen that the front emitter doping mainly influenced the solar cell efficiency by current.

From the result it can be seen clearly that on the rear side a large gain in V_{oc} is expected for reduced surface concentration, while the benefit in Isc is only marginal. Therefore the BSF mainly influence the efficiency by limited voltage.

It is also found that between high and low surface concentration shows different phenomena. Normally, BSF roles of internal reflection and carrier collection at the rear side, and the barrier on the carrier transport can be reduced by increasing the doping concentration, which explains the high doping concentration is guarantee of good BSF. (Al screen printing BSF) But in low surface concentration, since it is no heavily doped rear side, V_{oc} quickly increased and lower surface concentration provides less recombination.

The reduction of rear doping at the same time increases the requirements for the rear passivation and metallization. And the

limitation of ohmic contact problem also needs to be concerned. V_{OC} potential of this cell is mainly limited by a high amount of dopant in the silicon. It is demonstrated that the heavily doped rear side is limiting the implied V_{OC}. High quality rear side passivation can unlock the full V_{OC} potential. Meanwhile, a sufficiently high surface concentration (> 10^{20} cm^3) is also necessary to achieve low ohmic rear side contacts. Now most of companies are using the pastes which are able to provide low contact resistance and low phosphorous doped surfaces to solve this problem.

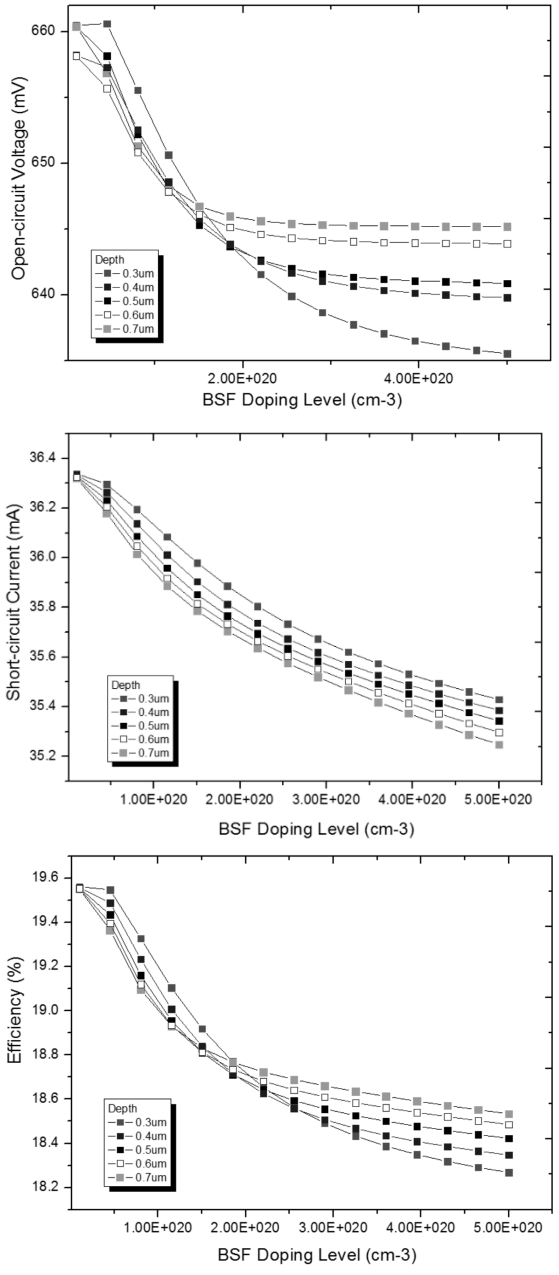

Fig. 11. PC1D simulation for cell performance depending on doping profiles of BSF

The comparison of emitter and BSF doping profiles indicates that the cell current is determined by the front emitter doping while the cell voltage is mainly limited by the rear side doping.

4. N-type bifacial solar cell design

For the investigation, the n-type bifacial solar cell fabrication process flow is shown in Fig. 12. 6 inch wide pseudo-square <100> *n*-type Cz mono-Si wafers with a bulk resistivity of 1-3Ω cm and a thickness of 170-200 um were used as substrates. The main variation between the three process flows was the BSF formation method. After a standard saw damage removal and

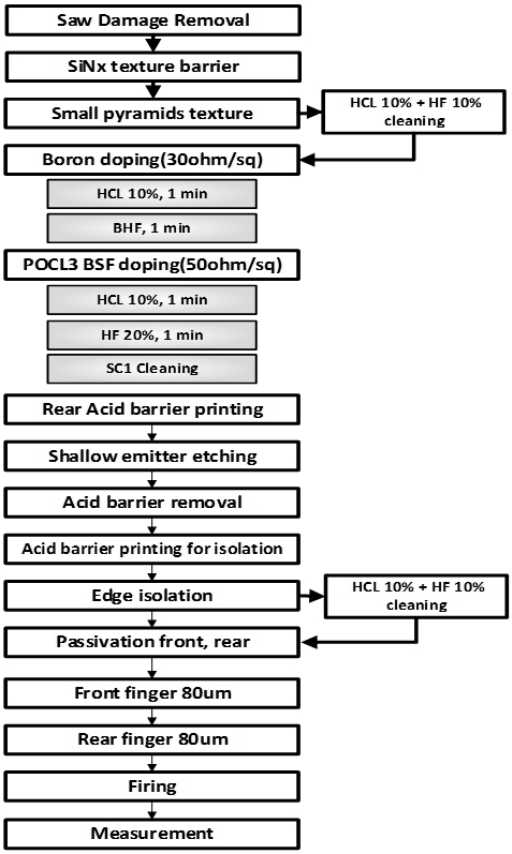

Fig. 12. N-type bifacial solar cell fabrication flow chart

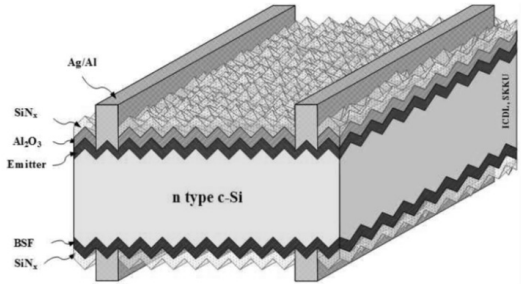

Fig. 13. N-type bifacial solar cell structure

texturing process, the wafers were diffused in different batches in a standard tube diffusion furnace of boron for the emitter formation and phosphorous for the back surface field (BSF) formation. After phosphorus silicate glass (PSG) removal using diluted HF, an Al_2O_3 layer was deposited by ALD and a SiONx layer by PECVD on the emitter surface while a SiNx layer was deposited on the BSF for rear side surface passivation and anti-reflection coating (ARC). A standard industrial screen printing process was applied using Al/Ag paste for the front contact and Ag paste for the rear contact on a standard screen print line. Finally the samples were co-fired in an industrial inline fast firing furnace (Fig. 12).

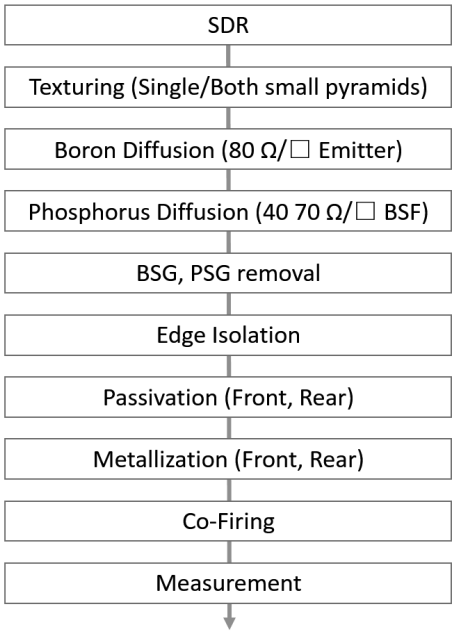

BBr3 doping process for Emitter

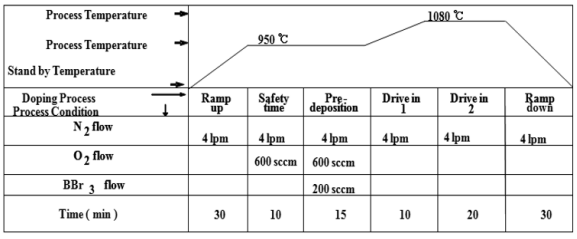

Doping Process / Process Condition	Ramp up	Safety time	Pre-deposition	Drive in 1	Drive in 2	Ramp down
N_2 flow	4 lpm	4 lpm	4 lpm	4 lpm	4 lpm	4 lpm
O_2 flow		600 sccm	600 sccm			
BBr_3 flow			200 sccm			
Time (min)	30	10	15	10	20	30

$POCl_3$ doping process for BSF

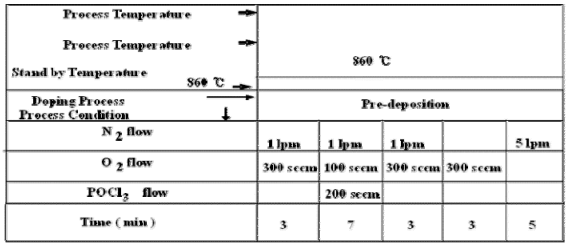

Doping Process / Process Condition	Pre-deposition				
N_2 flow	1 lpm	1 lpm	1 lpm		5 lpm
O_2 flow	300 sccm	100 sccm	300 sccm	300 sccm	
$POCl_3$ flow		200 sccm			
Time (min)	3	7	3	3	5

Fig. 14. Definition of the process flow for Emitter and BSF doping profile

For an n-type c-Si substrate a p-type layer acts as emitter and an n-type layer acts as BSF (Back surface field). A thermal diffusion is commonly used for emitter and BSF diffusion. After the diffusion process at front and rear sides, the edge isolation was carried out, as otherwise the top and the bottom surfaces of the wafers remain electrically shorted.

The diffusion depends on various factors, of which temperature and gaseous environment is most important. The homogeneity of the sheet resistance over the wafer and over the tube position may vary, depending on the amount of wafers. The second high temperature step also influences the dopant distribution of the initial diffusion step. The doping distribution is hence defined by the combined thermal budget as well as the surface capping layer (Fig. 14).

The main variation between the each process flows was the BSF formation method. We compare two different BSF profiles (40, 70 Ω/□), chemical cleaning treatment and several different passivation and metallization methods. All wafers were saw damage etched and boron emitter diffusion was subsequently divided into three groups to process phosphorus BSF doping. The first one was the standard diffusion profile and achieved a sheet resistance of 70 Ω/□ using a PSG pre-deposition at 830°C and sheet resistance of 40 Ω/□ using a PSG pre-deposition at 860°C. The second group BSF LD1 was added with in-situ pre-oxidation before the PSG pre-deposition step. This oxide layer acts as a diffusion barrier, minimizing the amount of phosphorus diffusion into silicon. In addition, the oxidation creates self-interstitials at the surface of the silicon to reduce the diffusion rate of phosphorus. The third group BSF LD2 was

Phosphorus BSF doping profile						
Sheet resistance	40Ω/□			70Ω/□		
Doping profile	STD BSF	BSF LD1	BSF LD2	STD BSF	BSF LD1	BSF LD2
Process 1	Pre-deposition	in-situ pre-oxidation	Pre-deposition	Pre-deposition	in-situ pre-oxidation	Pre-deposition
Process 2		Pre-deposition	Multilevel drive-in plateau		Pre-deposition	Multilevel drive-in plateau

Fig. 15. Phosphorus BSF doping profile

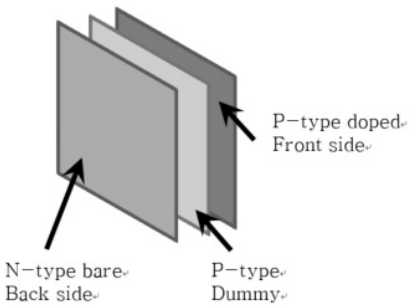

Fig. 16. Back to back $POCl_3$ doping method p-type dummy wafer put inside between two n-type wafers

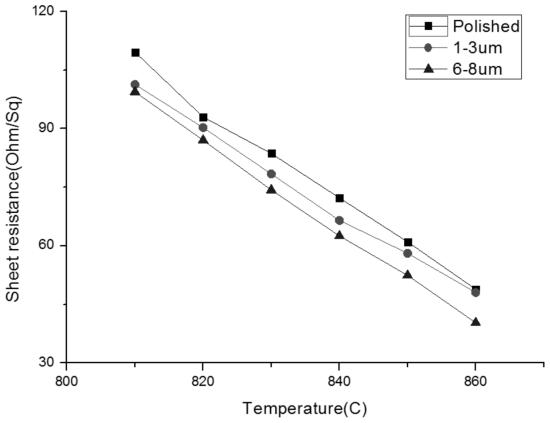

Fig. 17. Relationship between sheet resistance and temperature of $POCl_3$ pre-deposition diffusion for BSF

added with a multilevel drive-in plateau followed by a separate oxidation/drive-in after PSG removal with the same sheet resistance but deeper junction depth (Fig. 15).

5. Conclusions

In this paper, studies have been carried out on the optimization of phosphorus BSF on n-type bifacial solar cells, such as surface dopant concentration, doping depth, surface recombination and contact problems. A lightly phosphorus doped BSF (LD BSF) was optimized to get low surface dopant concentration for n-type bifacial solar cells. Pre-oxidation combined with a multi-plateau drive-in, using limited source diffusion was carried out before pre-deposition.

A lightly phosphorus doped BSF (LD BSF) method was achieved by optimizing the doping profile to get lower surface dopant concentration. The method is a pre-oxidation process before pre-deposition was combined with a multi-plateau drive-in, using limited source diffusion techniques. It could reduce the surface dopant concentration with minimal impact on the sheet resistance to investigate the n-type bifacial solar cell rear side phosphorus-doped BSF formation.

Acknowledgments

This work was supported by the New & Renewable Energy Technology Development Program of the Korea Institute of Energy Technology Evaluation and Planning (KETEP) grant funded by the Korea government Ministry of Trade, Industry & Energy.

References

1. D. M. Chapin, C. S. Fuller, and G. L. Pearson. A New Silicon p-n Junction Photocell for Converting Solar Radiation into Electrical Power. Journal of Applied Physics, 25 (5):676, 1954.
2. J. E. Cotter, et al. "P-type versus n-type Silicon Wafers: Prospects for High-Efficiency Commercial Silicon Solar Cells." IEEE Transactions on Electron Devices, 53(8):1893-1901, 2006.
3. S. W. Glunz, S. Rein, J. Y. Lee, and W. Warta. "Minority carrier lifetime degradation in boron-doped Czochralski silicon." Journal of Applied Physics, 90(5):2397, 2001.
4. J. Schmidt, et al. "N-type silicon - The better material choice for industrial high efficiency solar cells." In Proceedings of the 22th European Photovoltaic Solar Energy Conference and Exhibition, 2007.
5. J. Schmidt and K. Bothe, "Structure and transformation of the metastable boron- and oxygen-related defect center in crystalline silicon," Physical Review B, vol. 69, no. 2, Article ID 024107, pp. 241071-241078, 2004.
6. S. W. Glunz, S. Rein, J. Y. Lee, and W. Warta, "Minority carrier lifetime degradation in boron-doped Czochralski silicon," Journal of Applied Physics, vol. 90, no. 5, pp. 2397-2404, 2001.
7. J. Schmidt, A. G. Aberle, and R. Hezel, "Investigation of carrier lifetime instabilities in Cz-grown silicon," in Proceedings of the 1997 IEEE 26th Photovoltaic Specialists Conference, pp. 13-18, October 1997.
8. D. Macdonald and L. J. Geerligs, "Recombination activity of interstitial iron and other transition metal point defects in p and n-type crystalline silicon," Applied Physics Letters, vol. 85, no. 18, pp. 4061-4063, 2004.
9. Fabian Kiefer, et al, "Influence of the boron emitter profile on VOC and JSC losses in fully ion implanted n-type PERT solar cells." Phys. Status Solidi A 212, No. 2, 291-297 (2015).
10. Vinodh Shanmugam et al., "Electrical and Microstructural Analysis of Contact Formation on Lightly Doped Phosphorus Emitters sing Thick-Film Ag Screen Printing Pastes," IEEE JOURNAL OF PHOTOVOLTAICS, VOL. 4, NO. 1, 2014.
11. J. Schmidt, J. Bothe, R. Bock, C. Schmiga, R. Krain, and R. Brendel. "N-type silicon - The better material choice for industrial high efficiency solar cells." In Proceedings of the 22th European Photovoltaic Solar Energy Conference and Exhibition, 2007.
12. S. P. Phang and D. Macdonald. "Direct comparison of boron, phosphorus, and aluminum gettering of iron in crystalline silicon." Journal of Applied Physics, 109(7):073521, 2011.
13. M. Rüdiger, C. Schmiga, M. Rauer, M. Hermle, and S. W. Glunz. "Efficiency Potential of n-Type Silicon Solar Cells with Aluminum-Doped Rear p+ Emitter." IEEE Transactions on Electron Devices, 59(5):1295-1303, May 2012.
14. F. Book, T. Wiedenmann, G. Schubert, H. Plagwitz, and G. Hahn. "Influence of the Front Surface Passivation Quality on

Large Area n-Type Silicon Solar Cells with Al-Alloyed Rear Emitter." Energy Procedia, 8:487-492, 2011.

15. J. Zhao, A. Wang, and M. A. Green. "24.5% Efficiency silicon PERT cells on MCZ substrates and 24.7% efficiency PERL cells on FZ substrates." Progress in Photovoltaics: Research and Applications, 7(6):471-474, November 1999.
16. J.Benick, S.W. Glunz, et al. "High efficiency n-type Si solar cells on Al_2O_3-passivated boron emitters." Applied Physics Letters, 92(25):253504, June 2008.
17. J. Benick, B. Hoex, et al. "High-Efficiency n-Type Silicon Solar Cells with Front Side Boron Emitter." In Proceedings of the 24th European Photovoltaic Solar Energy Conference, pages 863-870. WIP-Munich, November 2009.
18. J. Zhao, J. Schmidt, A. Wang, Guangchun Z., B. S. Richards, and M. A. Green. "Performance instability in n-type PERT silicon solar cells." In Proc. 31st IEEE Photovoltaic Specialists Conf. (PVSC), volume 1, pages 923-926 Vol.1, 2003.
19. A. Richter, J. Benick, A. Kalio, J. Seiffe, M. Hörteis, M. Hermle, and S. W. Glunz. "Towards industrial n-type PERT silicon solar cells: rear passivation and metallization scheme." Energy Procedia, 8:479-486, January 2011.
20. S. Bordihn, P. Wawer, et al. "Large area n-type Cz double side contacted back junction boron emitter solar cell." In Proceedings of the 26th European Photovoltaic Solar Energy Conference and Exhibition, 2011.
21. V. Mertens, J.W. Müller, et al. "Large Area n-Type Cz Double Side Contact Back Junction Solar Cell with 21.3% Conversion Efficiency." In Proceedings of the 28th European Photovoltaic Solar Energy Conference and Exhibition, 2013.
22. N. Guillevin, J. Xiong, et al., "High Power n-Type Metal-Wrap-through Cells and Modules Using Industrial Processes." In Proceedings of the 28th European Photovoltaic Solar Energy Conference and Exhibition. WIP, 2013.
23. D. Kania, H.-J. Krokoszinski, et al., "Pilot Line Production of Industrial High-Efficient Bifacial n-type Silicon Solar Cells with Efficiencies Exceeding 20.6%." In Proceedings of the 28th European Photovoltaic Solar Energy Conference and Exhibition, 2013.
24. J.-B. Heng, Z. Xu, et al., "Commercialization of Tunnel Oxide Junction Based Cell and Module with Efficiency and Good Reliability." In Proceedingsofthe28thEuropeanPhotovoltaic Solar Energy Conference and Exhibition, 2013.
25. R. Woehl, M. Rüdiger, D. Biro, and J. Wilde. "All-screen-printed back-contact backjunction silicon solar cells with aluminum-alloyed emitter and demonstration of interconnection of point-shaped metalized contacts." Progress in Photovoltaics: Research and Applications, pages n/a–n/a, September 2013.
26. D. D. Smith, D. Vicente, et al. "Generation III high efficiency lower cost technology: Transition to full scale manufacturing." In Proc. 38th IEEE Photovoltaic Specialists Conf. (PVSC), pages 001594–001597. IEEE, June 2012.
27. F.Feldmann, M.Bivour.C.Reichel, M.Hermle, S.W.Glunz. "A passivated Rear contact for high efficiency n-type silicon solar cells enabling high Voc and FF>82%."